Water Research 290 (2026) 124996

Contents lists available at ScienceDirect

Water Research

journal homepage: www.elsevier.com/locate/watres

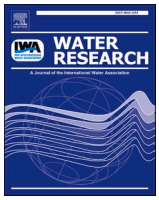

Formation of regulated and novel disinfection by-products during chlorine and chlorine dioxide disinfection of surface water and groundwater

Maolida Nihemaiti [a,*], Jon Wullenweber [b,c], Mattia Stefanoni [d], Laura Kahle [a], Oliver J. Lechtenfeld [a], Beatrice Cantoni [d], Manuela Antonelli [d], Mathias Ernst [b,c], Thorsten Reemtsma [a,e]

[a] Helmholtz Centre for Environmental Research - UFZ, Department of Environmental Analytical Chemistry, Permoserstraße 15, 04318 Leipzig, Germany
[b] Hamburg University of Technology, Institute for Water Resources and Water Supply, Am Schwarzenberg-Campus 3, 21073 Hamburg, Germany
[c] DVGW Research Centre TUHH, Am Schwarzenberg-Campus 3, 21073 Hamburg, Germany
[d] Politecnico di Milano, Department of Civil and Environmental Engineering, Piazza Leonardo da Vinci, 32, 20133 Milano, Italy
[e] Institute for Analytical Chemistry, University of Leipzig, Linnéstrasse 3, 04103 Leipzig, Germany

HIGHLIGHTS

- More sulfonated DBPs formed from samples with higher S- and N-containing DOM.
- Sulfonated DBPs originate from different precursors than regulated THMs.
- The studied groundwater shows more heteroatom-DOM as sulfonated DBP precursors.
- ClO_2 produces more non-chlorinated, heteroatom-containing DBPs than chlorine.

ARTICLE INFO

Keywords:
Chlorination
Trihalomethanes
Drinking water
DBP precursors
Dissolved organic matter
Non-target analysis

ABSTRACT

The formation of disinfection by-products (DBPs) during water disinfection is a health concern. A limited number of DBPs, such as trihalomethanes (THMs), are regulated and used as indicators of human exposure to the broader group of DBPs. However, it remains poorly understood whether the formation mechanisms and precursors of unregulated DBPs are similar to that of regulated ones. In this study, lab-scale chlorination and chlorine dioxide (ClO_2) disinfection were conducted on four different source waters (two surface water and two groundwaters). DBP formation was assessed through targeted analysis of THMs via gas chromatography-mass spectrometry, novel sulfonated DBPs via supercritical fluid chromatography-mass spectrometry, and non-targeted analysis using liquid chromatography coupled to Fourier transform ion cyclotron resonance mass spectrometry (LC-FT-ICR-MS). The formation of THMs during chlorination was higher in surface waters (49–111 μg per mg dissolved organic carbon, DOC, at 48 h) than in groundwaters (21–27 μg per mg DOC) and corresponded to their higher initial specific UV-absorbance ($SUVA_{254}$) and higher humic acid fractions as determined by LC-organic carbon detection. ClO_2 disinfection led to significantly lower THM levels (below the limit of detection of 0.20 μg/L) across all samples. Similarly, the formation of sulfonated DBPs was one order of magnitude lower. However, unlike THMs, sulfonated DBPs were formed to a greater extent in both groundwaters (3.0–3.6 μg per mg DOC) than in surface waters (2.0–2.2 μg per mg DOC), suggesting that sulfonated DBPs are preferentially formed from other precursors than THMs. This was further elucidated by LC-FT-ICR-MS analysis showing that the higher levels of sulfur- and nitrogen- containing dissolved organic matter in the studied groundwater samples likely contributed to the increased formation of sulfonated DBPs. Furthermore, LC-FT-ICR-MS analysis outlined that disinfection by ClO_2, while reducing halogenated DBPs, resulted in even higher levels of non-chlorinated, sulfur- and nitrogen-containing DBPs. In conclusion, strategies focused on reducing regulated THMs may be insufficient to mitigate the formation of sulfonated and other novel heteroatom-containing DBPs during drinking water treatment.

* Corresponding author.
E-mail address: maolida.nihemaiti@ufz.de (M. Nihemaiti).

https://doi.org/10.1016/j.watres.2025.124996
Received 3 June 2025; Received in revised form 12 November 2025; Accepted 17 November 2025
Available online 17 November 2025

1. Introduction

Disinfection is a critical step to prevent waterborne disease from drinking water. Chemical disinfectants (e.g., chlorine-based compounds, chlorine dioxide) can react with natural organic matter (NOM), anthropogenic organic compounds, bromide, and iodide in the water matrices to form disinfection byproducts (DBPs) (Richardson et al., 2007). The formation of DBPs is undesired as DBP exposure can be linked with adverse health effect, such as birth defect and bladder cancer in humans (Couri et al., 1982; Costet et al., 2011; Wright et al., 2017; Weisman et al., 2022). Over 700 DBPs have been identified to date, most of which are low molecular weight, volatile compounds amenable to analysis by gas chromatography-mass spectrometry (GC–MS). These DBPs, however, only account for about 30 % of total halogenated products formed during chlorination (Hua and Reckhow, 2007).

Four trihalomethanes (THM4: chloroform, bromodichloromethane, dibromochloromethane, and bromoform) and a small number of other DBPs are regulated in many countries. The European Union has set limits on THM4 (100 μg/L), five haloacetic acids (HAAs, 60 μg/L), bromate (10 μg/L), chlorite (0.25 mg/L), and chlorate (0.25 mg/L) (European Union, 2020). DBP regulation is based on the assumption that the regulated DBPs are the indicators of exposure to the complex mixtures of all DBPs in disinfected water (Li and Mitch, 2018). However, many unregulated DBPs, such as haloacetonitriles, haloacetamides, and haloacetaldehydes, are proven to be more toxic than the regulated ones (Wagner and Plewa, 2017) and the main toxicity drivers in disinfected water still remain unknown (Richardson and Plewa, 2020).

With advances in analytical technologies, previously unknown DBPs are being revealed. Reversed-phase liquid chromatography coupled to MS (RPLC-MS) is increasingly applied to identify higher molecular weight DBPs (>2 carbons) (Mitch et al., 2023). Particularly, the combination of RPLC with high resolution MS, such as quadrupole time-of-flight (QTOF) and Orbitrap, facilitates the identification of novel DBPs by providing accurate mass and structural information (Wawryk et al., 2021). Fourier transform ion cyclotron resonance MS (FT-ICR-MS) can be a powerful tool for molecular level characterization of complex organic matter, owing to its unrivalled resolution, mass accuracy and sensitivity (Reemtsma, 2009). FT-ICR-MS is used to study the molecular level change of dissolved organic matter (DOM) upon various disinfection processes, which is useful to understand the reaction mechanisms and precursors, as well as to identify novel DBPs (Andersson et al., 2023). The coupling of FT-ICR-MS with liquid chromatography (LC-FT-ICR-MS) allows to analyze more polar fractions of DOM (Han et al., 2021) and has recently been applied to analyze DBPs (Han et al., 2023).

Despite its wide application in various DBP studies, RPLC-MS analysis, however, can result in analytical gaps by overlooking the extremely polar fractions of DBPs as these compounds are hardly retained on RP columns (e.g., C18) (Reemtsma et al., 2016). Therefore, alternative chromatographic separation methods like hydrophilic interaction chromatography (HILIC) and supercritical fluid chromatography (SFC) can be useful to narrow such analytical gaps in analyzing polar DBPs.

Zahn et al. recently employed HILIC-Orbitrap-MS to identify halomethanesulfonic acids in chlorinated drinking water, with concentrations detected in the low μg/L range (Zahn et al., 2019). Furthermore, Nihemaiti et al. applied SFC-QTOF-MS to reveal that the sulfonic acid derivatives of all regularly monitored haloacetonitriles, haloacetamides, and haloacetaldehydes are present in finished water from drinking water treatment plants (DWTPs) as well as in tap water samples, with concentrations ranging from tens to hundreds of ng/L (Nihemaiti et al., 2023). These newly found sulfonated DBPs are extremely polar and may pose health risks due to their structural similarity to toxic DBPs. However, little is known about their precursors and formation mechanisms in complex water matrices. Furthermore, it remains unclear whether the formation potential of sulfonated DBPs correlates with the formation of regulated DBPs under different disinfection conditions. Such information is essential to learn about how the formation of sulfonated DBPs can be avoided.

In this study, we aim to understand the potential relationship between the formation of 20 novel sulfonated DBPs vs. the regulated DBPs (THM4, chlorite, and chlorate) as a function of the presence and characteristics of NOM. Disinfection tests were conducted using sodium hypochlorite (NaOCl) and chlorine dioxide (ClO_2) on four water matrices (two synthetic waters prepared with surface water model NOM and two treated groundwater samples). Changes in NOM during disinfection were characterized using absorbance, liquid chromatography-organic carbon detection (LC-OCD), and LC coupled with FT-ICR-MS. In addition, non-target analysis of DBPs was performed using LC-FT-ICR-MS to generally investigate the characteristics of DBPs formed from different water matrices during the two disinfection processes.

2. Material and methods

2.1. Chemicals

All chemicals were of analytical grade and used as received without further purification. Sodium hydroxide (≥99 %), hydrochloric acid (15 %), potassium dihydrogen phosphate (≥99 %), sodium bisulfite solution (>37 %, in water), sodium thiosulfate pentahydrate (≥99.5 %), and sodium hypochlorite solution (12 %) were obtained from Carl Roth (Karlsruhe, Germany). Diethyl phenylenediamine sulfate (DPD) salt was purchased from Hach Lange (EU) and used through a DPD dispenser (DPD Free Chlorine Reagent, Swiftest™ Dispenser). Carbon dioxide Premium (4.5) was used for SFC. Methanol, acetonitrile, and formic acid were purchased from Biosolve (Valkenswaard, Netherlands). Sodium dichloromethanesulfonate (97 %) and sodium dibromomethanesulfonate (>95 %) were purchased from Toronto Research Chemicals. Ultrapure water was obtained from a Merck Milli-Q Integral 5 system (Darmstadt, Germany). A ClO_2 stock solution (2 $gClO_2$/L) was weekly prepared by the Oxiperm® Pro OCD-162 generator (5 $gClO_2$/h, Grundfos, IT) using sodium chlorite and hydrochloric acid, both technical grade (Chimitex, IT); it was stored in headspace-free amber glass vials at 4 °C.

2.2. Water samples

Four different water matrices (two synthetic waters and two groundwater samples) were used for disinfection experiments (Table 1). The synthetic waters were prepared either by dissolving Suwannee River natural organic matter (SRNOM) extract or by diluting a sample from

Table 1
The composition and properties of water samples used in this study.

Water samples [a]	Composition	DOC (mg/L)	SUVA m^{-1} $(mg/L)^{-1}$
SRNOM	Suwannee River NOM extract	3	3.5
HSNOM	Diluted Hohlohsee lake water	3	4.9
GW1	Groundwater treated by aeration, sand filtration, and deacidification	3.4	2.5
GW2	Groundwater treated by granular activated carbon filtration	0.2	1.6

[a] All samples were buffered with 10 mM phosphate buffer at pH 7.

Hohlohsee (HSNOM). SRNOM represents river/swamp-derived NOM, while HSNOM serves as an example of lake-derived NOM. The SRNOM isolate (2R101N) was obtained from International Humic Substances Society (IHSS, USA) and prepared according to Wullenweber et al. (2024). Hohlohsee is a bog lake based in a conversation zone in an upland moor in the Black Forest, Germany. A batch sample (ID HO31) of Hohlohsee, containing >20 mg/L dissolved organic carbon (DOC), was kindly provided by Engler-Bunte-Institute Karlsruhe (Karlsruhe, Germany) and was extensively characterized elsewhere (Frimmel et al., 2002). HSNOM was prepared by diluting this sample with ultrapure water until DOC of 3 mg/L.

Two groundwater samples (GW1 and GW2) with different DOM composition and DOC content were also used for disinfection experiments. GW1 was collected from a DWTP located in northern Germany, the source water of which is derived from a mix of shallow and deep wells that extract water from aquifers primarily composed of sands, lignite-derived sands, and gravel. The sample was collected immediately after aeration, sand filtration, and deacidification processes at the DWTP. GW2 was collected from a DWTP located in northern Italy, fed on a cluster of about 20 wells. It was a deep groundwater (~50 m, mainly gravel and sand sediments with the presence of clay-silt layers) treated by granular activated carbon (GAC, bituminous microporous activated carbon, iodine number: 900–1000 mg/g) filters with an empty bed contact time of 11 min.

All water samples were filtered using a 0.45 μm filter to remove undissolved substances and large particles. The pH was subsequently adjusted to 7.0 ± 0.2 using 0.1 M NaOH and 0.1 M HCl, and phosphate buffer (10 mM, pH 7) according to APHA standard 5710 (APHA, 2017).

2.3. NaOCl and ClO_2 disinfection experiments

All experiments were performed in chlorine-demand and headspace-free, brown glassware at room temperature (20 ± 2 °C). The predetermined volume of disinfectant stock solution (i.e., NaOCl or ClO_2) was spiked into water samples to get an initial chlorine dosage of 5 mg/L as Cl_2, that is equivalent to an initial ClO_2 concentration of 1.92 mg/L, assuming a conversion ratio of 2.63 $mgCl_2/mgClO_2$ based on the oxidative potential of the two disinfectants (White, 2010). After the disinfectant addition, sample bottles were immediately inverted to mix and incubated for 0.5, 2, 6, 24, and 48 h (individual bottle per contact time). After each contact time, the residual disinfectant was determined using: (i) in NaOCl disinfection experiments, standard cuvette tests (LCK 410), (ii) in ClO_2 disinfection experiments, DPD colorimetric method (4500-Cl.G), using potassium permanganate solution as standard (APHA, 2017).

After each contact time, an aliquot of samples was quenched and directly analyzed for THMs, dichloromethanesulfonic acid (Cl_2MSA), dibromomethanesulfonic acid (Br_2MSA), chlorite and chlorate (only in the case of ClO_2 experiments), and DOM characterization through absorbance. For the analysis of THMs, samples were quenched with sodium thiosulfate, while sodium bisulfite quencher was used for the analyses of Cl_2MSA and Br_2MSA. Nitrogen gas was bubbled through the sample for 1 min as a quenching reagent in case of chlorite and chlorate analysis. Additional samples after 48 h were collected without quenching to analyze other sulfonic DBPs using SFC-QTOF-MS following freeze-drying enrichment. Furthermore, samples before and after 48 h were analyzed without quenching using LC-OCD by direct injection and LC-FT-ICR-MS following freeze-drying enrichment to characterize the change in DOM composition.

2.4. Analysis of THMs

Samples were analyzed using a GC–MS/MS (QP2020 NX, Shimadzu) according to EPA method 5030C (2003) and 8260D (2018) (USEPA, 2003, 2018). The limit of detection (LOD) is 0.20 μg/L. Details of GC–MS operation conditions are given in the supporting information (Text S1).

2.5. Analysis of chlorite and chlorate

Samples were analyzed applying an ion chromatography coupled to a UV/Vis detector (944 Professional UV/VIS Detector Vario, Metrohm, Switzerland) using a Metrosep A Supp 7 - 250/4.0 column and a Metrosep A Supp 10 Guard HC/4.0 pre-column. The method followed for the analyses is the APAT- IRSA/CNR 4020 Man 29/2003. The LOD is 75 μg/L.

2.6. Analysis of sulfonated DBPs

Total 20 sulfonated DBPs, which are the chloro- and bromo-analogues of halomethanesulfonic acids, haloacetonitrilesulfonic acids, haloacetamidesulfonic acids, and haloacetaldehydesulfonic acids were studied (Table 2). Among them, Cl_2MSA and Br_2MSA are with analytical standards, therefore quantified using a SFC-TQXS-MS. Other sulfonated DBPs were analyzed using a SFC-QTOF-MS based on signal intensities.

Quantification of Cl_2MSA and Br_2MSA. Samples were directly injected to an ACQUITY UPC2® system coupled with a Xevo® TQ-XS-MS (Waters, Germany). The analytes were separated using a Viridis BEH column (3.0 mm × 100 mm, 1.7 μm, Waters, Germany) with an injection volume of 5 μL. The mobile phase consisted of CO_2 and a methanol/ultrapure water (95:5, by volume) co-solvent containing 10 mM ammonium formate. To transfer the column effluent into the mass spectrometer, a methanol/ultrapure water (90:10, by volume) makeup flow containing 0.1 % formic acid with a flow rate of 0.3 mL/min was used. The analytes were ionized using electrospray ionization (ESI) in negative mode. The analysis was performed in MRM mode using two transitions per analyte (Table S1). Details of method are given in Text S2.

Analysis of other sulfonated DBPs. A previous study showed that certain nitrogen-containing sulfonated DBPs were unstable in the presence of quenching reagents (Nihemaiti et al., 2023). Therefore, no additional chemical was added to quench the residual chlorine or ClO_2 prior to SFC-QTOF analysis of samples after 48 h disinfection. Samples were enriched by freeze-drying before injection to SFC-QTOF-MS. The apparent recovery rates of sulfonated DBPs during freeze-drying enrichment were thoroughly investigated in a previous study (Nihemaiti et al., 2023). In that study, mixtures of sulfonated DBPs at various concentrations were spiked into different water samples with varying DOC levels. The results showed that freeze-drying provided complete recoveries for chloroacetonitrilesulfonic acid (ClANSA, 100 ± 10 %) and dichloroacetonitrilesulfonic acid (Cl_2ANSA, 99 ± 7 %), whereas relatively lower recovery was observed for dichloroacetaldehydesulfonic acid (Cl_2AcAlSA, 43 ± 10 %). However, no clear dependence of the apparent recovery rates on the water matrix or spiked concentration was observed (Nihemaiti et al., 2023). A 40 mL aliquot of each sample was filled in a 50 mL centrifuge tube and stored at −20 °C overnight. The frozen sample was then placed in a freeze-dryer (Alpha1–4, Christ, Germany) at 15 °C and 1.65 mbar for 30 h until dryness. The residue was reconstituted in 400 μL of acetonitrile and water (90:10, by volume), transferred into an Eppendorf tube, and then centrifuged at 13,000 min^{-1} for 10 min. The supernatant was then

Table 2
The sulfonated DBPs investigated in this study [a].

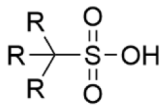	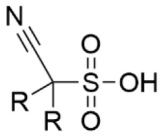	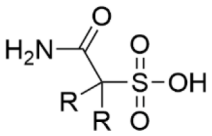	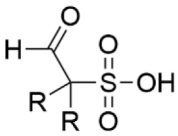
Halomethanesulfonic acids	Haloacetonitrilesulfonic acids	Haloacetamidesulfonic acids	Haloacetaldehydesulfonic acids
Chloromethanesulfonic acid (ClMSA) Dichloromethanesulfonic acid (Cl_2MSA) Bromochloromethane sulfonic acid (BrClMSA) Bromomethanesulfonic acid (BrMSA) Dibromomethanesulfonic acid (Br_2MSA)	Chloroacetonitrilesulfonic acids (ClANSA) Dichloroacetonitrilesulfonic acid (Cl_2ANSA) Bromochloroacetonitrilesulfonic aicd (BrClANSA) Bromoacetonitrilesulfonic acid (BrANSA) Dibromoacetonitrilesulfonic acid (Br_2ANSA)	Chloroacetamidesulfonic acids (ClAcAmSA) Dichloroacetamidesulfonic acids (Cl_2AcAmSA) Bromochloroacetamidesulfonic acid (BrClAcAmSA) Bromoacetamidesulfonic acid (BrAcAmSA) Dibromoacetamidesulfonic acid (Br_2AcAmSA)	Chloroacetaldehydesulfonic acids (ClAcAlSA) Dichloroacetaldehydesulfonic acids (Cl_2AcAlSA) Bromochloracetaldehydesulfonic acids (BrClAcAlSA) Bromoacetaldehydesulfonic acids (BrAcAlSA) Dibromoacetaldehydesulfonic acid (Br_2AcAlSA)

[a] R in chemical structures represents H, Cl, or Br.

transferred into glass vials and kept at −20 °C until analysis. The samples were analyzed using an ACQUITY UPC2 system coupled with a Synapt GS2 QTOF-MS (Waters, Germany) in negative ESI mode. The SFC parameters were similar to the SFC-TQXS analysis mentioned above. Following settings were applied on the QTOF-MS: capillary voltage: 2 kV, source temperature 120 °C, desolvation temperature 600 °C, and desolvation gas flow 1000 L/h. Nitrogen and argon are used as cone and collision gases, respectively. The data was recorded in centroid mode with a 0.1 per second scan time over the mass range of *m/z* 50–1200 (resolution approximately 20,000). The MS^E acquisition was performed to simultaneously collect two data sets: a low-collision-energy scan to obtain parent ion information and an elevated-collision-energy scan (15–40 eV) to get all fragment ions. Data is processed using Waters MassLynx and TargetLynx software. The retention time and mass spectrometric data of sulfonated DBPs are given in Table S2.

2.7. Analysis of UV absorbance and DOC

The absorbance at 254 nm (UV_{254}) was measured (1 cm optical path) using a UV–VIS DR6000 spectrophotometer (Hach Lange, Düsseldorf, Germany) in ClO_2 experiments, and a UV–VIS DR5000 spectrophotometer (Hach Lange GmbH, Düsseldorf, Germany) in NaOCl experiments. DOC was determined using a TOC analyzer (Shimadzu, Japan).

2.8. LC-OCD analysis

Organic carbon composition was analyzed by size-exclusion chromatography using an LC-OCD system from DOC Labor Huber (Karlsruhe, Germany), with a column packed with Toyopearl HW 50 S resin (Tosoh Bioscience, Tokyo, Japan), which allows distinguishing between the chromatographic organic carbon separated into five different fractions and the non- chromatographic organic carbon classified as hydrophobic organic carbon. The definition of the chromatographic organic carbon fractions is described in the supporting information (Text S3) and illustrated in Fig. S1. The LC-OCD system is equipped with both an organic carbon detector (OCD) and a UV detector (UVD, 254 nm). A sample volume of 2 mL was regularly injected; for samples with DOC < 0.5 mg/L 4 mL was injected. The measurement procedure is extensively described elsewhere (Huber et al., 2011).

2.9. LC-FT-ICR-MS analysis

To avoid interference with instrumental analysis and potential interactions with DOM or DBPs (Fu et al., 2022; Andersson et al., 2023), no quenching reagent was applied prior to LC-FT-ICR-MS analysis. Aliquots (40 mL) of the samples before and after 48 h of disinfection were enriched by freeze-drying following the same procedure mentioned in Section 2.6 and reconstituted in 1 mL of ultrapure water, resulting in a nominal enrichment factor of 40. Freeze-drying was chosen as an enrichment method to retain the highly polar fractions of DOM and DBPs, which are often partially lost during SPE-based methods (Jennings et al., 2022; Han et al., 2023), and to ensure consistency across both targeted and non-targeted DBP analyses in this study. Moreover, freezing has been shown to have a low impact on the composition of organic matter (<10 %) (Fonvielle et al., 2023). Samples were analysed in negative ESI mode with FT-ICR-MS (SolariX XR, Bruker Daltonics Inc., Billerica, MA, USA) coupled to a UHPLC system (UltiMate 3000RS, Thermo Fischer Scientific, Waltham, MA, USA) following a method published previously (Han et al., 2021; Jennings et al., 2022).

Chromatographic data were segmented into one minute bins between 12 and 24 min ($n = 12$), mass spectra ($n = 30$/bin) averaged and internally calibrated with a list of commonly detected DOM masses (*m/z* 150–980, $n = 425$) using Compass DataAnalysis (version 5.0, Bruker Daltonics). Molecular formula (MF) were assigned to mass peaks with signal-to-noise (S/N) ≥ 4 using the elemental composition of $C_{1–80}$, $^{13}C_{0–1}$, $H_{1–198}$, $O_{0–40}$, $N_{0–2}$, $S_{0–1}$, $^{34}S_{0–1}$, $^{35}Cl_{0-3}$, $^{37}Cl_{0–2}$ within the mass tolerance of ± 0.42 ppm. Br was not included for the assignments as this element is currently not available in the Lambda-Miner (Wurz et al., 2024). Multiple assignments were reduced using mass error distributions according to Gao et al. (2024). Signals were assigned as Cl-DBP if absent in process blanks or in samples before disinfection and for which the $^{35}Cl_n$-$^{37}Cl_1$ peak magnitude ratio was within the 25th (0.75) and 75th (1.17) percentile of $^{35}Cl_n$-$^{37}Cl_1$ peak magnitude (Han et al., 2023). Finally, other, non-chlorinated DPB were identified as MF present only in samples after disinfection for which the S/N ratio was larger than the 5th percentile of S/N ratios from DOM MF before disinfection (4.26). A feature is defined as a molecular formula in a specific retention time segment. For visualization purposes retention-time segments were intensity averaged into a single mass spectrum. For an overview on the

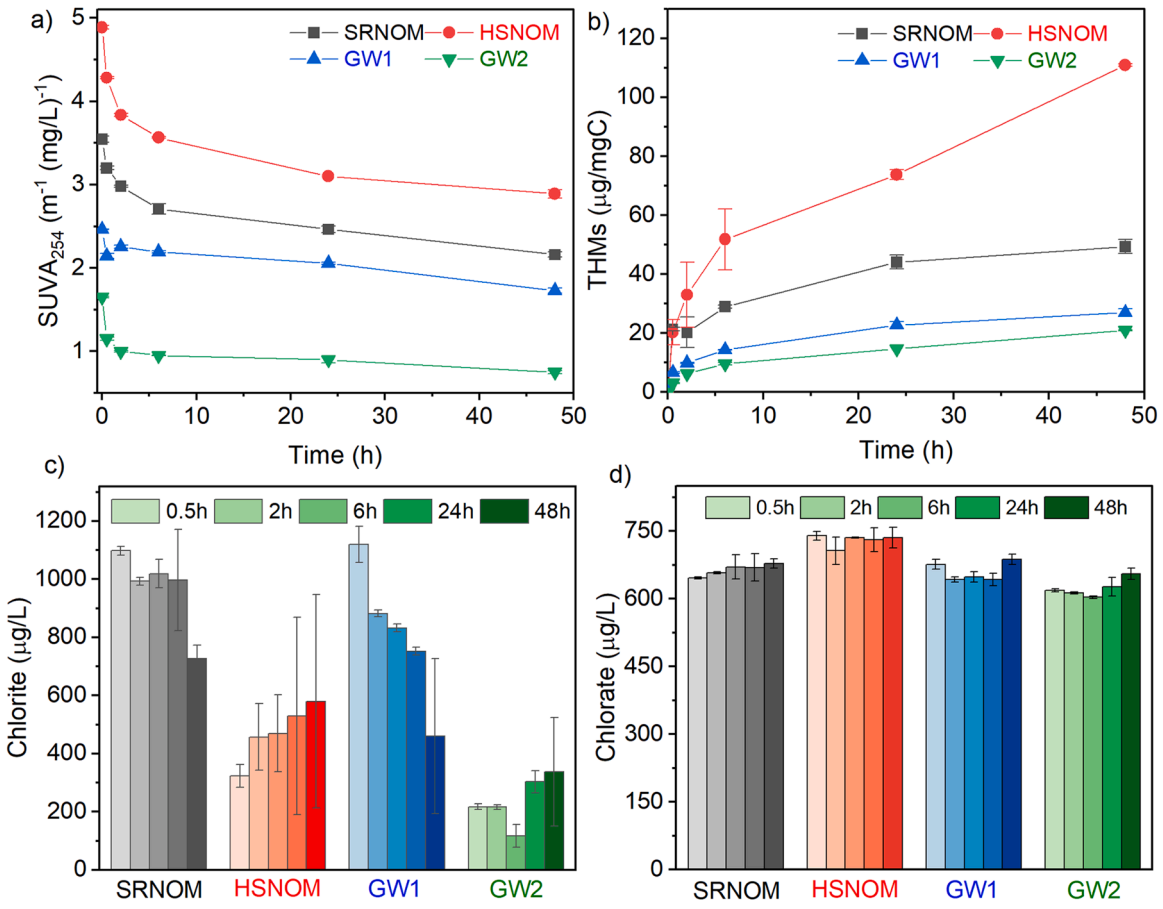

Fig. 1. The kinetics of (a) $SUVA_{254}$ reduction and (b) THM4 formation (normalized per mg initial DOC) during chlorination, as well as the formation of (c) chlorite and (d) chlorate during ClO_2 disinfection of four water samples. Initial NaOCl or ClO_2 concentration: 5 mg/L as Cl_2. All samples were buffered with 10 mM phosphate buffer at pH 7. Error bars represent the standard deviation of duplicate experiments. Within each sample in (c) and (d), the color gradient from light to dark corresponds to increasing reaction time (0.5, 2, 6, 24, and 48 h).

data processing, refer to Fig. S2.

Disinfection experiments and LC-FT-ICR-MS analysis were performed in duplicate, representing technical replicates. Most samples were measured with the same ion accumulation time (IAT) of 50 ms, except for GW2, where higher IATs (i.e., 100, 250, or 500 ms) were applied due to its very low DOC concentration (Table S3). Results for all replicates are provided in Tables S3–6; however, only one replicate per sample was used for the graphs shown in Sections 3.3 and 3.4. Technical replicates measured with the same IAT yielded comparable numbers of MFs and similar distributions across formula classes (Table S3). For samples with comparable IATs (SRNOM, HSNOM, and GW1), the percentage of shared chlorinated DBPs (i.e., identical MFs detected in both replicates) ranged from 53 % for GW1 (719 Cl-DBPs in total) to 36 % for HSNOM during chlorination (Tables S4–5).

3. Results and discussions

3.1. Formation of regulated DBPs

The chlorination and ClO_2 disinfection of four water samples were performed for up to 48 h and the residual disinfectants, UV_{254} absorption, and DBPs were analyzed simultaneously as a function of reaction time. During chlorination, the residual chlorine in all water samples gradually decreased over time (Fig. S3a), featuring a rapid reduction in the first 6 h followed by a slower reduction rate (Kastl et al., 1999; Deborde and von Gunten, 2008). Chlorine consumption was highest for HSNOM (residual chlorine: 0.9 mg/L as Cl_2 after 48 h) and lowest in GW2 (residual chlorine: 4.8 mg/L as Cl_2 after 48 h), the sample with the lowest DOC content (0.2 mg/L; Table 1). The extent of chlorine consumption aligns with the distinct $SUVA_{254}$ values of the matrices (Fig. 1a), indicating that humic substances underwent rapid reactions with chlorine and were significantly transformed (Weishaar et al., 2003).

THM formation during chlorination was also rapid at the beginning and then slowed down (Fig. 1b). HSNOM produced the highest THM yield after 48 h (111 μg per mg DOC), whereas GW2 had the lowest THM yield (21 μg per mg DOC). Overall, a higher initial $SUVA_{254}$ corresponded to a higher chlorine consumption and, finally, a higher THM formation (Hua et al., 2015).

During ClO_2 disinfection, the degradation of ClO_2 was much more rapid than that of chlorine and almost completed (> 95 %) within the first 0.5 h (Fig. S3b), except for GW2 (residual ClO_2: 0.7 mg/L as Cl_2 at 48 h) with a low DOC content. No THMs were detectable in any sample during ClO_2 disinfection, reflecting the lower THM formation potential

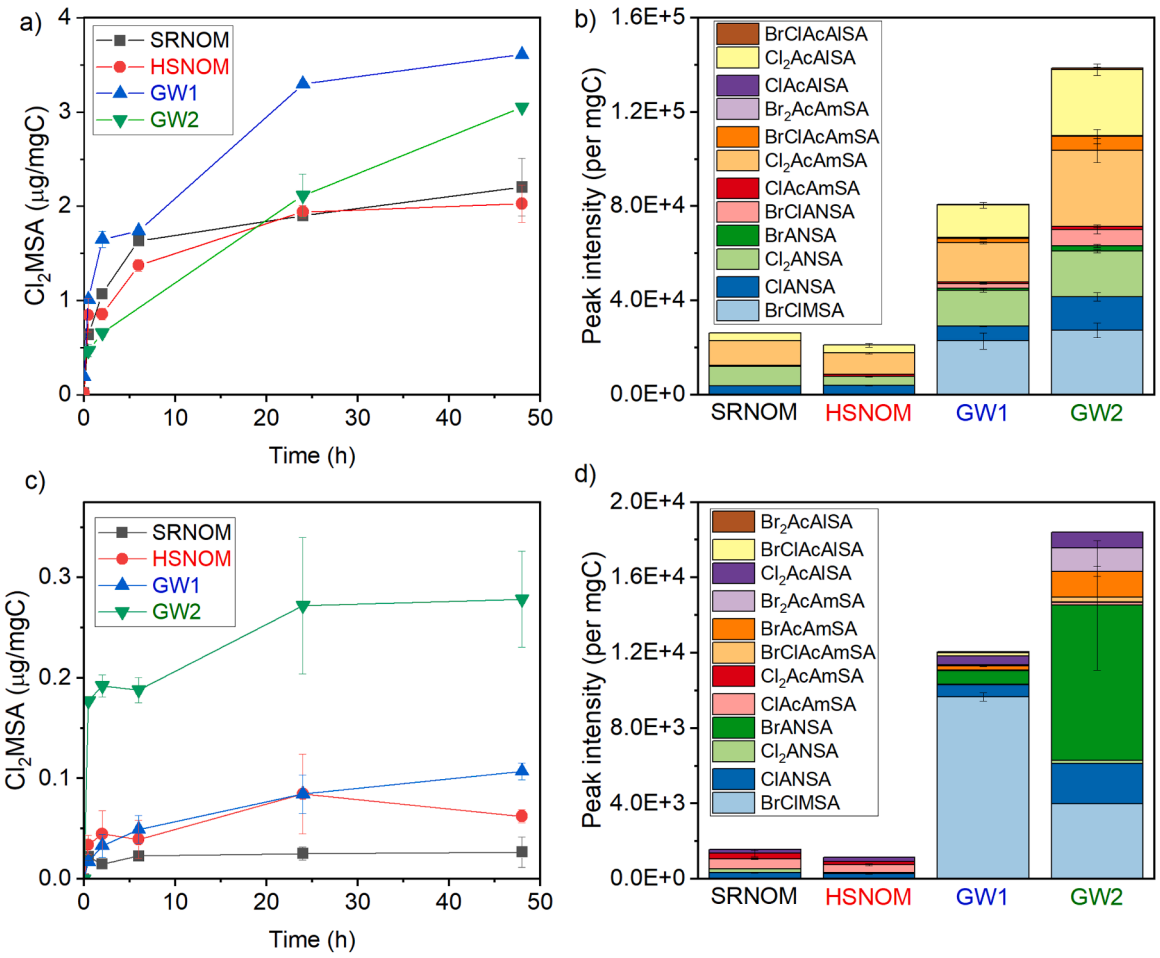

Fig. 2. The formation kinetics of Cl_2MSA (normalized per mg DOC) from four water samples during chlorination (a) and ClO_2 disinfection (c); Intensities (normalized per mg DOC) of other sulfonated DBPs after 48 h of chlorination (b) and ClO_2 disinfection (d). Initial NaOCl or ClO_2 concentration: 5 mg/L as Cl_2. All samples were buffered with 10 mM phosphate buffer at pH 7. Error bars represent the standard deviation of duplicate experiments. For full names of DBPs, refer to Table 2.

from ClO_2 as compared to chlorine (Hua and Reckhow, 2007). Chlorite was rapidly produced in the first 0.5 h in all samples, although to different extent (Fig. 1c); for SRNOM and GW1, the chlorite level was already high (~ 1100 μg/L) at 0.5 h, and then decreased, while for HSNOM and GW2, the initial level was much lower (200 – 300 μg/L) and then showed an increasing trend until 48 h. Chlorite is produced during ClO_2 oxidation via a one-electron transfer from organic moieties to ClO_2 (Gordon et al., 1972). The lower formation of chlorite in GW2 was possibly related to its much lower DOC concentration (i.e., fewer organic moieties) as compared to the other samples (0.2 vs. ~ 3 mg/L; Table 1). Previous studies have shown that the yield and kinetics of chlorite formation depend on the distribution of ClO_2-reactive functional groups in DOM (e.g., amines, olefins, phenolic substances) (Gan et al., 2019). Certain functional groups with strong nucleophilicity (e.g., thiols) can further reduce chlorite to chloride ion (Ison et al., 2006). Therefore, more detailed characterization of DOM functional groups in each sample would be required to explain the observed chlorite formation behaviour. Unlike chlorite, the chlorate levels of all four samples were similar from the beginning and remained almost stable (~ 650 μg/L, Fig. 1d). This suggests that chlorate formation is not directly related to organic matter but rather to the natural disproportionation of ClO_2 (Gordon et al., 1972). Overall, the formation yields of chlorite (12 – 58 %) and chlorate (26 %) observed in this study were within the similar range of previous lab-scale ClO_2 oxidation of model compounds and NOM isolates (Rougé et al., 2018; Gan et al., 2019).

3.2. Formation of novel sulfonated DBPs

Formation of Cl_2MSA during chlorination was observed for all four water samples (Fig. 2a), with concentration increasing rapidly in the beginning and then slowing down gradually until 48 h. Interestingly, GW1 and GW2 tended to produce more Cl_2MSA (3.6 and 3.0 μg per mg DOC, respectively) compared to SRNOM and HSNOM (2.2 and 2.0 μg per mg DOC, respectively). This is contrary to the formation trend of THMs mentioned above (Fig. 1b), suggesting that Cl_2MSA and THMs originate from different precursors.

Moreover, the formation of Cl_2MSA also did not follow the trend of residual chlorine and $SUVA_{254}$: HSNOM water, which presented the highest chlorine consumption and UV_{254} reduction, had a low Cl_2MSA yield, indicating that Cl_2MSA formation was independent on the chlorine consumption and $SUVA_{254}$ in these water samples.

Additional samples were taken after 48 h of chlorination and enriched by freeze-drying to increase the sensitivity of detection. ClANSA, Cl_2ANSA, chloro-, dichloroacetamidesulfonic acids (ClAcAmSA, $Cl_2AcAmSA$), and $Cl_2AcAlSA$ were detected from all samples (Fig. 2b). The brominated analogues of these DBPs (BrANSA, BrClANSA,

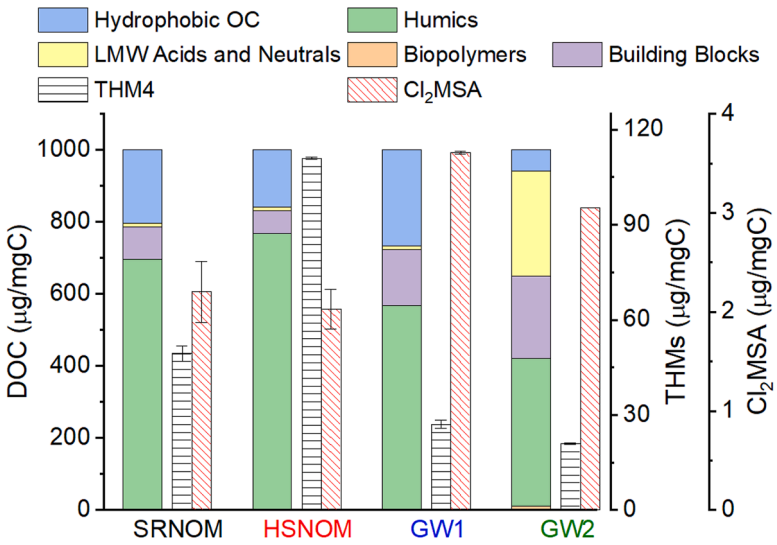

Fig. 3. The DOM fractions obtained from LC-OCD analysis of non-disinfected water samples, as well as the concentrations of THM4 and Cl_2MSA after 48 h of chlorination. Error bars represent the standard deviation of duplicate experiments.

BrClAcAmSA, $Br_2AcAmSA$, BrClAcAlSA) as well as bromochloromethanesulfonic acid (BrClMSA) and Br_2MSA, were also detected from GW1 and GW2. This is attributed to the presence of naturally occurring bromide in groundwater (95 µg/L in GW1). Bromide can be rapidly oxidized by chlorine to hypobromous acid (HOBr), which can further react with NOM to produce brominated DBPs (Hua et al., 2006). No bromide was added to SRNOM and HSNOM samples. Br_2MSA was quantified using SFC-TQXS-MS, which gave 200 ng/L in GW1 after 48 h of chlorination and under detection limit in GW2 (LOD: 20 ng/L). The sum of the intensities of sulfonated DBPs per mg DOC were much higher in GW1 and GW2 as compared to SRNOM and HSNOM. These findings further support above suggestion that the two groundwater samples contained more precursors of sulfonated DBPs than the NOM isolate from river (SRNOM) and the diluted lake water (HSNOM).

About 10–50 times less Cl_2MSA was produced during ClO_2 disinfection as compared to chlorination (Fig. 2c). Also the total peak intensity of all other sulfonated DBPs was about one order of magnitude lower than after chlorination (Fig. 2d). These results suggest that ClO_2 produces not only less THMs, but also less sulfonated DBPs. The majority of Cl_2MSA was formed in the first 0.5 h of the reaction with little further increase. This can be explained by the fast depletion of ClO_2 within the first 0.5 h (Fig. S3b). The formation of Cl_2MSA per mg DOC was ~3 times higher in GW2 than in other samples.

Similar to chlorination, ClO_2 also produced the sulfonic acid derivatives of chloromethanes, chloroacetonitriles, chloroacetamides, and chloroacetaldehydes (Fig. 2d). Furthermore, ClO_2 is known to not react with bromide (Hoigné and Bader, 1994); however, the in situ formed free chlorine during ClO_2 disinfection can oxidize bromide to HOBr, which reacts with DOM to produce brominated DBPs (Rougé et al., 2018). In agreement with this, the brominated analogues of sulfonated DBPs were also detected from GW1 and GW2. The sum of the intensities (per mg DOC) of all sulfonated DBPs were much higher in GW1 and GW2 than in SRNOM and HSNOM samples. These results are consistent with the chlorination experiments mentioned above that these groundwater samples appeared to contain more precursors of sulfonated DBPs.

3.3. Characterization of DOM using LC-OCD and LC-FT-ICR-MS

To understand the difference in the formation potentials of the regulated DBPs and the novel sulfonated DBPs during both NaOCl and ClO_2 disinfection, samples before and after 48 h were analyzed using LC-OCD.

The LC-OCD chromatograms of the non-disinfected samples showed a typical distribution of chromatographic organic carbon for HSNOM, SRNOM, and GW1, with the main fraction consisting of humic substances (HS), followed by a shoulder of building blocks (BB) and a peak corresponding to low-molecular-weight (LMW) acids and LMW HS (Fig. S4). In contrast, GW2 presented only a minor HS peak lacking a significant UV_{254} signal, indicative of reduced HS. This was followed by BB and a pronounced peak at LMW acids elution time, combined with a strong UV_{254} signal, suggesting the presence of mainly LMW HS (Huber et al., 2011) (Fig. S1). This is possibly because GW2 was treated by GAC, which led to the reduction of some HS.

HS accounted for the largest fraction of DOM in all four investigated water matrices, but in varying proportions. In HSNOM, HS comprised about 75 % of the total DOM, decreasing to 41 % in GW2. This trend aligns with the varying THM formation yields observed in these water samples (Fig. 3), in accordance with literature that humic substances are the major precursors of THMs (Nikolaou et al., 2004; Ibrahim et al., 2016). Moreover, disinfection induced distinct changes in DOM composition over 48 h of reaction time. Especially for HSNOM sample, a significant decrease in HS peak combined with a shift to higher elution times and an increase in BB and LMW-Acids/ -HS were visible (Fig. S5). This reflects the transformation of HS of higher MW into low MW substances. However, the proportion and transformation of HS observed via LC-OCD analysis cannot explain the formation trend of Cl_2MSA (Fig. 3). Therefore, LC-FT-ICR-MS was applied to further characterize DOM in each water sample at molecular level.

Samples before and after 48 h of chlorination or ClO_2 disinfection were analyzed using LC-FT-ICR-MS after freeze-drying enrichment. Between 7100 and 33400 molecular features were detected in each sample

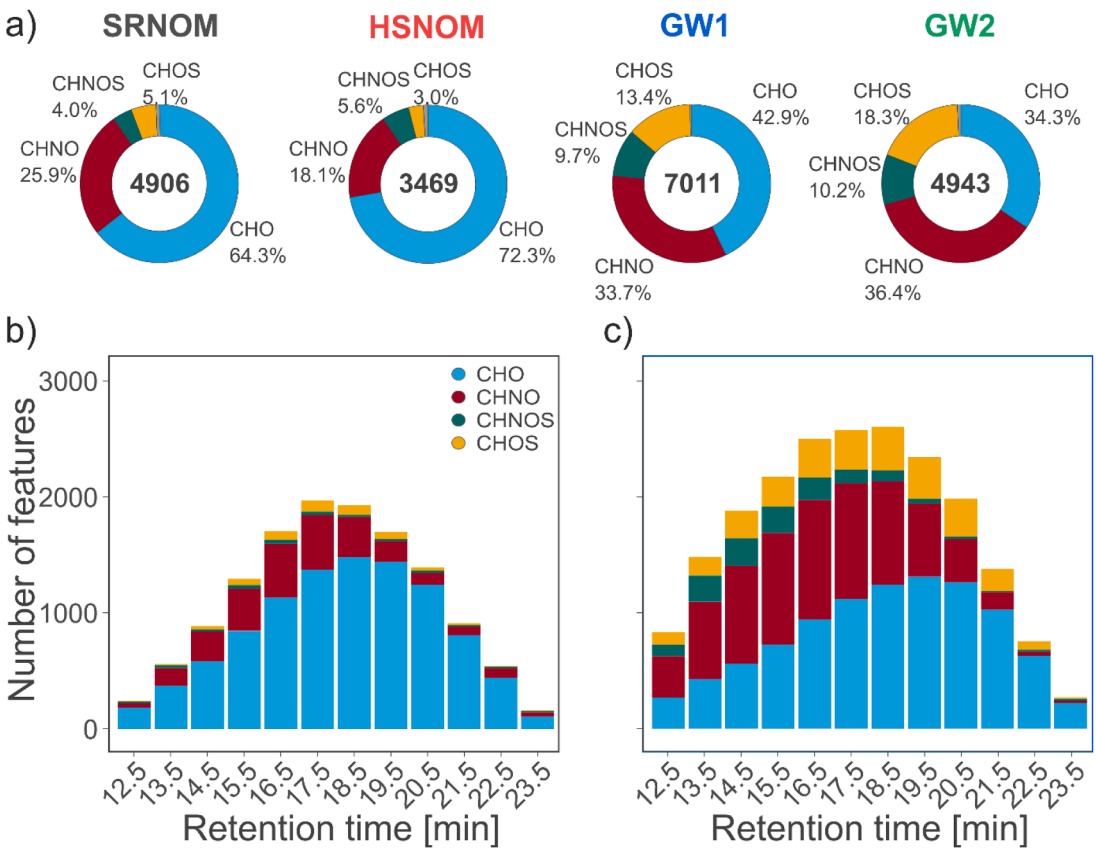

Fig. 4. The LC-FT-ICR-MS derived molecular formulas (MF) from four water samples. Distribution of MF classes in samples (prior to disinfection). a) Number (value in center) and fraction of unique MF in SRNOM, HSNOM, GW1, and GW2 according to the main formula classes (CHO: blue; CHNO: red; CHNOS: cyan; CHOS: yellow; all others: gray). Number of features in SRNOM (b) and GW1 (c) according to their reversed-phase retention time (decreasing polarity with increasing retention time). A "feature" represents a MF detected at a distinct retention time segment. The same MF can be detected multiple times across the chromatographic run and is only counted once for (a). Only data from the first replicate is shown. MF of the class "other" have abundances < 1 %.

matrix before disinfection, representing 3469 to 7011 unique molecular formulas (MFs) (Fig. 4a and Table S3). The number of detected signals and distribution of MF classes varied according to the DOM source. Both groundwater samples showed a larger number of MF, and a larger contribution of heteroatom-containing MF (CHNO, CHNOS, CHOS), with up to 67 % in GW1 compared to only 28 % in HSNOM (Fig. 4a and Table S3). The high abundance of heteroatom-containing MFs in groundwater reflects the selective sorption of plant-derived compounds onto mineral surfaces and the predominance of microbially processed organic matter released from deeper soil layers (Kaiser and Kalbitz, 2012; Roth et al., 2019; McDonough et al., 2022). The lower abundance of heteroatom-containing MFs in SRNOM may also be related to the incomplete recovery of these compounds during the isolation procedures used to prepare the NOM extract from Suwannee River water (e.g., reverse osmosis concentration, cation-exchange desalting, etc.) (Green et al., 2015).

Although the overall distribution of MF (classes) according to the RPLC polarity gradient was similar across all four samples with a maximum of abundance between 17 and 19 min retention time, CHNO and CHNOS class MFs eluted earlier while CHO and CHOS class MFs were shifted to higher retention times in groundwater samples as compared to SRNOM and HSNOM (Fig. 4b, c and Figs. S6, 7, 8). Thus, the CHO class of MF represents less polar DOM compounds, while CHNO and CHNOS represent more polar DOM compounds, particularly in groundwater. Sulfur-containing MFs (CHOS) span the entire range of polarity.

These results offer an explanation for the stronger formation of novel sulfonated DBPs (Section 3.2 and Table 2) from the two groundwater samples: they are enriched in sulfur- and nitrogen-containing NOM moieties as potential sulfonated DBP precursors. This hypothesis aligns with previous studies showing that model compounds containing thiol and sulfonated groups such as cysteine, glutathione, and *p*-phenolsulfonic acid can form these sulfonated DBPs upon chlorination (Nihemaiti et al., 2023). Studying the formation potential of sulfonated DBPs from a larger number of samples with parallel FT-ICR-MS analysis is needed to support this hypothesis.

3.4. Non-targeted characterization of chlorinated and non-chlorinated DBPs via LC-FT-ICR-MS

To further understand the difference in the formation trend of overall DBPs from surface and groundwater matrices upon two different disinfection processes, non-targeted analysis of DBPs was performed in the LC-FT-ICR-MS data. A large number of chlorinated DBPs (Cl-DBPs; between 244 in HSNOM to 572 in GW2) with up to 3 Cl atoms (Fig. 5c, d and Tables S4, 5) were detected after NaOCl disinfection. Most (>78 %) of Cl-DBPs were attributed to the CHO class, with a minor fraction of heteroatom-containing Cl-DBPs (Fig. 5c, d and Tables S4, 5). Cl-DBPs had similar molecular descriptors (Fig. 5c, d and Figs. S9, 10) as the CHO class, their likely precursors (Fig. 5a, b; Figs. S6, 7, 8, and 11). Overall, 82 sulfur-containing Cl-DBPs were detected with LC-FT-ICR-MS across all samples (Tables S4, 5), with 73 of them detected in GW 2. The novel sulfonated DBPs described in Section 3.2 were not detected by LC-FT-ICR-MS likely because of their extremely high polarity. Future studies could further elucidate the identities of the DBPs detected by LC-FT-ICR-MS through tandem MS analysis (Postigo et al., 2021).

Also, a large number (*n*: 330–1822) and fraction of heteroatom-

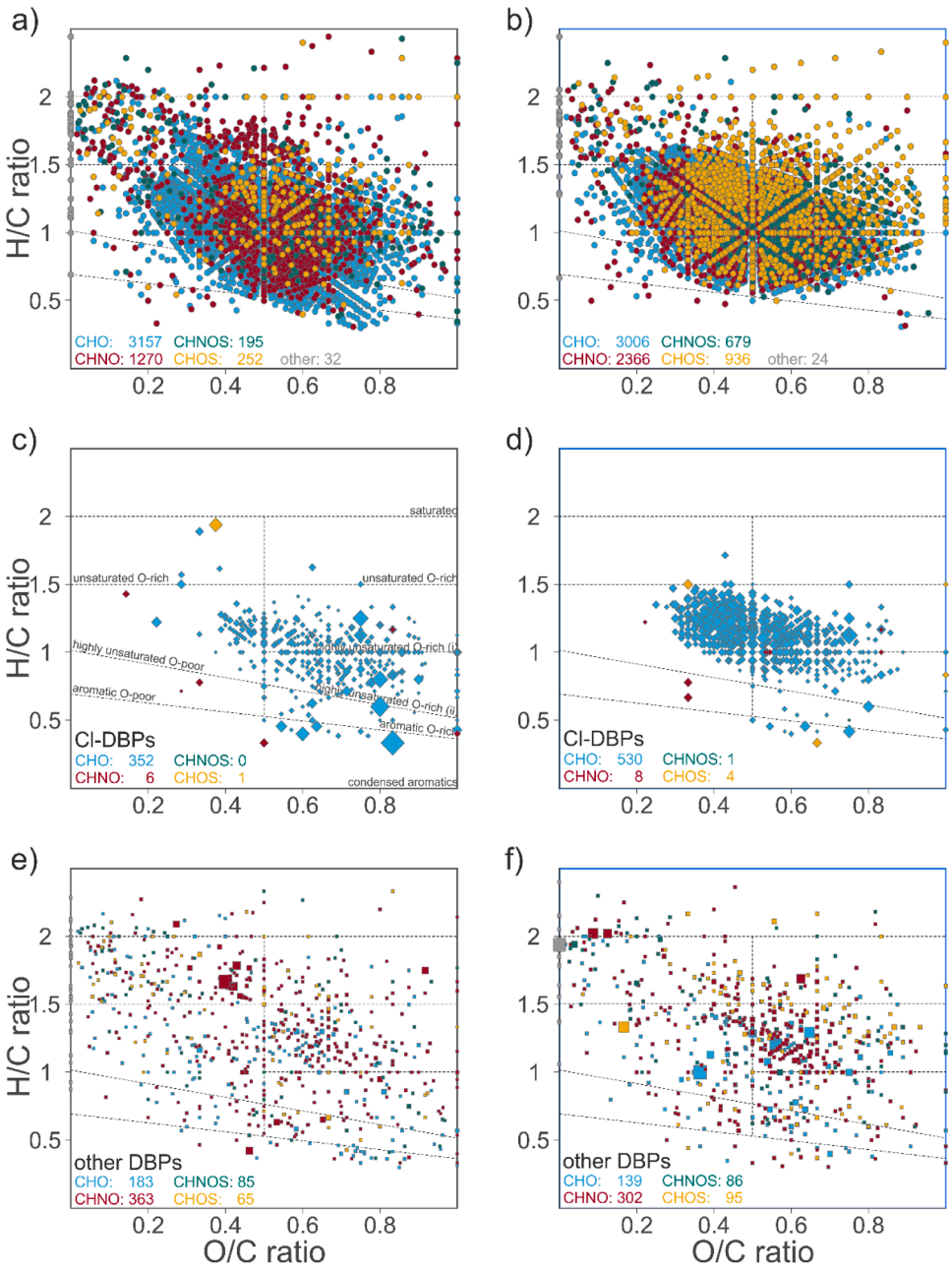

Fig. 5. DOM and DBP composition of surface (SRNOM) and groundwater (GW1) samples. Distribution of MFs in SRNOM (a, c, e) and GW1 (b, d, f) pre-disinfection (a, b) and DBPs after 48 h of NaOCl disinfection (c, d, e, f) according to their molecular hydrogen-to-carbon (H/C) and oxygen-to-carbon (O/C) ratios. Formula class (CHO: blue; CHNO: red; CHNOS: cyan; CHOS: yellow; all others: gray), and DBP class (diamonds: Cl-DBPs with 1–3 Cl atoms, c), d); squares: other DBPs without chlorine, e), f)). The number of each formula (and DBP) class and compound classes (names in c)) is indicated within each panel. DOM-MF and DBP-MF of the class "other" have abundances < 5 % and only data from the first replicate is shown.

containing, non-chlorinated DBPs (CHNO, CHNOS, CHOS: 66–77 % of all non-chlorinated DBPs) was detected after NaOCl disinfection, and their formula class distribution was comparable across samples (Table S6). Notably, the proportion of heteroatom-containing, non-chlorinated DBPs was larger than the initial fraction of heteroatom-containing DOM in these samples before disinfection, highlighting the role of heteroatoms in NOM for the formation of DBPs. The heteroatom containing, non-chlorinated DBPs may further be transformed into more toxic, chlorinated or brominated DBPs in the presence of residual disinfectants especially in drinking water distribution networks (Andersson et al., 2021).

Fewer chlorinated DBPs (7 in GW1 to 329 in HSNOM) (Table S4, 5) were detected after ClO_2 disinfection, consistent with previous studies indicating that ClO_2 generates less organic halogens than chlorination (Hua and Reckhow, 2007; Wang et al., 2024). But ClO_2 disinfection led to an even larger number of sulfur- and nitrogen-containing, non-chlorinated DBPs (*n*: 381–2392; 51–81 %) as compared to NaOCl (Table S6). This is likely because, unlike chlorine, which reacts with organic compounds via oxidation, addition, and substitution (Deborde and von Gunten, 2008), ClO_2 reacts selectively with electron-rich moieties (e.g., phenols, amines, thiols) primarily through electron-transfer reactions (Gan et al., 2020). As a result, less halogenated, but more sulfur- and nitrogen-containing non-halogenated DBPs were produced by ClO_2 disinfection than chlorination.

Overall, more sulfur- and nitrogen-containing, non-chlorinated DBPs were detected on a number basis in GW1 and GW2 during both

disinfection processes, reflecting the higher number of heteroatom-containing DOM in theses samples as compared to SRNOM and HSNOM (Fig. 4a). Notably, in GW1, a much larger number of sulfur- and nitrogen-containing DBPs was found after ClO_2 as compared to NaOCl disinfection (Fig. S12).

4. Conclusions

- Sulfonated DBPs were formed from all groundwater as well as surface water samples during both chlorination and ClO_2 disinfection. Their trend of formation did not follow the regulated THMs during chlorination, suggesting that the precursors of sulfonated DBPs might differ from that of THMs.
- The formation of regulated THMs can be predicted using generic parameters such as chlorine demand, $SUVA_{254}$ values, and LC-OCD analysis, whereas novel sulfonated DBPs defy such predictions.
- Molecular-level characterization of DOM using LC-FT-ICR-MS suggests that samples with higher levels of sulfur- and nitrogen-containing DOM tend to produce greater amounts of sulfonated DBPs, as well as non-targeted heteroatom-containing, non-chlorinated DBPs, during both chlorination and ClO_2 disinfection.
- ClO_2 disinfection can effectively reduce the formation of halogenated DBPs, but produces more non-halogenated, heteroatom-containing DBPs than chlorination.
- Strategies aiming at reducing the formation of regulated THMs during drinking water treatment may be insufficient to mitigate the formation of sulfonated and other novel DBPs.

Funding

This research was funded by the European Union under grant agreement No 101,081,980 (project SafeCREW). Views and opinions expressed are however those of the author(s) only and do not necessarily reflect those of the European Union or European Research Executive Agency. Neither the European Union nor the granting authority can be held responsible for them.

CRediT authorship contribution statement

Maolida Nihemaiti: Writing – review & editing, Writing – original draft, Validation, Methodology, Investigation, Funding acquisition, Data curation, Conceptualization. **Jon Wullenweber:** Writing – review & editing, Writing – original draft, Methodology, Data curation, Conceptualization. **Mattia Stefanoni:** Writing – review & editing, Writing – original draft, Methodology, Investigation, Data curation. **Laura Kahle:** Investigation, Data curation. **Oliver J. Lechtenfeld:** Writing – review & editing, Writing – original draft, Validation, Investigation, Conceptualization. **Beatrice Cantoni:** Investigation, Funding acquisition, Conceptualization. **Manuela Antonelli:** Writing – review & editing, Supervision, Funding acquisition, Conceptualization. **Mathias Ernst:** Writing – review & editing, Supervision, Funding acquisition, Conceptualization. **Thorsten Reemtsma:** Writing – review & editing, Supervision, Funding acquisition, Conceptualization.

Declaration of competing interest

The authors declare that they have no known competing financial interests or personal relationships that could have appeared to influence the work reported in this paper.

Acknowledgements

The authors would like to thank Metropolitana Milanese Spa (Milan, Italy) for analyzing regulated DBPs. The authors are also grateful to Jan Kaesler, Fabian Carl, Bettina Seiwert, and Coretta Bauer at the UFZ for their assistance with instrumental analysis, and to Shuxian Gao at the UFZ for his support in data analysis.

Supplementary materials

Supplementary material associated with this article can be found, in the online version, at doi:10.1016/j.watres.2025.124996.

Data availability

Processed and quality checked LC-FT-ICR-MS data for all samples and segments are available from the UFZ Data Investigation Portal: https://doi.org/10.48758/ufz.16265. Raw MS files can be shared upon request.

References

Andersson, A., Gonsior, M., Harir, M., Hertkorn, N., Schmitt-Kopplin, P., Powers, L., Kylin, H., Hellström, D., Nilsson, K., Pettersson, Ä., Stavklint, H., Bastviken, D., 2021. Molecular changes among non-volatile disinfection by-products between drinking water treatment and consumer taps. Environ. Sci.: Water Res. Technol. 7 (12), 2335–2345.

Andersson, A., Harir, M., Bastviken, D., 2023. Extending the potential of Fourier transform ion cyclotron resonance mass spectrometry for the analysis of disinfection by-products. TrAC Trends Anal. Chem. 167, 117264.

APHA, 2017. Standard Methods for the Examination of Water and Wastewater, 23rd ed. American Public Health Association., Washington DC, USA.

Costet, N., Villanueva, C.M., Jaakkola, J.J.K., Kogevinas, M., Cantor, K.P., King, W.D., Lynch, C.F., Nieuwenhuijsen, M.J., Cordier, S., 2011. Water disinfection by-products and bladder cancer: is there a European specificity? A pooled and meta-analysis of European case–control studies. Occup Env. Med. 68 (5), 379–385.

Couri, D., Abdel-Rahman, M.S., Bull, R.J., 1982. Toxicological effects of chlorine dioxide, chlorite and chlorate. Env. Health Perspect. 46, 13–17.

Deborde, M., von Gunten, U., 2008. Reactions of chlorine with inorganic and organic compounds during water treatment—Kinetics and mechanisms: a critical review. Water Res. 42 (1), 13–51.

European Union (2020) Directive (EU) 2020/2184 of the European Parliament and of the Council of 16 December 2020 on the quality of water intended for Human consumption.

Fonvielle, J.A., Felgate, S.L., Tanentzap, A.J., Hawkes, J.A., 2023. Assessment of sample freezing as a preservation technique for analysing the molecular composition of dissolved organic matter in aquatic systems. RSC Adv. 13 (35), 24594–24603.

Frimmel, F.H., Abbt-Braun, G., Heumann, G.K., Hock, B., Lüdemann, H.-D., Spiteller, M., 2002. Refractory Organic Substances in the Environment. Wiley-VCH, Weinheim, Germany.

Fu, Q.-L., Fujii, M., Watanabe, A., Kwon, E., 2022. Formula assignment algorithm for deuterium-labeled ultrahigh-resolution mass spectrometry: implications of the formation mechanism of halogenated disinfection byproducts. Anal. Chem. 94 (3), 1717–1725.

Gan, W., Ge, Y., Zhong, Y., Yang, X., 2020. The reactions of chlorine dioxide with inorganic and organic compounds in water treatment: kinetics and mechanisms. Environ. Sci.: Water Res. Technol. 6 (9), 2287–2312.

Gan, W., Huang, S., Ge, Y., Bond, T., Westerhoff, P., Zhai, J., Yang, X., 2019. Chlorite formation during ClO2 oxidation of model compounds having various functional groups and humic substances. Water Res. 159, 348–357.

Gao, S., Jennings, E.K., Han, L., Koch, B.P., Herzsprung, P., Lechtenfeld, O.J., 2024. Detection and exclusion of false-positive molecular formula assignments via mass error distributions in UHR mass spectra of natural organic matter. Anal. Chem. 96 (25), 10210–10218.

Gordon, G., Kieffer, R.G. and Rosenblatt, D.H. (1972) The chemistry of chlorine dioxide. In Progress in Inorganic Chemistry, pp. 201–286.

Green, N.W., McInnis, D., Hertkorn, N., Maurice, P.A., Perdue, E.M., 2015. Suwannee River natural organic matter: isolation of the 2R101N reference sample by reverse osmosis. Env. Eng. Sci. 32 (1), 38–44.

Han, L., Kaesler, J., Peng, C., Reemtsma, T., Lechtenfeld, O.J., 2021. Online counter gradient LC-FT-ICR-MS enables detection of highly polar natural organic matter fractions. Anal. Chem. 93 (3), 1740–1748.

Han, L., Lohse, M., Nihemaiti, M., Reemtsma, T., Lechtenfeld, O.J., 2023. Direct non-target analysis of dissolved organic matter and disinfection by-products in drinking water with nano-LC-FT-ICR-MS. Environ. Sci.: Water Res. Technol. 9 (6), 1729–1737.

Hoigné, J., Bader, H., 1994. Kinetics of reactions of chlorine dioxide (OClO) in water—I. Rate constants for inorganic and organic compounds. Water Res. 28 (1), 45–55.

Hua, G., Reckhow, D.A., 2007. Comparison of disinfection byproduct formation from chlorine and alternative disinfectants. Water Res. 41 (8), 1667–1678.

Hua, G., Reckhow, D.A., Abusallout, I., 2015. Correlation between SUVA and DBP formation during chlorination and chloramination of NOM fractions from different sources. Chemosphere 130, 82–89.

Hua, G., Reckhow, D.A., Kim, J., 2006. Effect of bromide and iodide ions on the formation and speciation of disinfection byproducts during chlorination. Env. Sci. Technol. 40 (9), 3050–3056.

Huber, S.A., Balz, A., Abert, M., Pronk, W., 2011. Characterisation of aquatic humic and non-humic matter with size-exclusion chromatography – organic carbon detection – organic nitrogen detection (LC-OCD-OND). Water Res. 45 (2), 879–885.
Ibrahim, M.B.M., Radwan, E.K., Moursy, A.S., Bedair, A.H., 2016. Humic substances as precursors for trihalomethanes yields upon chlorination. Desalin. Water Treat. 57 (55), 26494–26500.
Ison, A., Odeh, I.N., Margerum, D.W., 2006. Kinetics and mechanisms of chlorine dioxide and chlorite oxidations of cysteine and glutathione. Inorg Chem. 45 (21), 8768–8775.
Jennings, E., Kremser, A., Han, L., Reemtsma, T., Lechtenfeld, O.J., 2022. Discovery of polar ozonation byproducts via direct injection of effluent organic matter with online LC-FT-ICR-MS. Env. Sci. Technol. 56 (3), 1894–1904.
Kaiser, K., Kalbitz, K., 2012. Cycling downwards – dissolved organic matter in soils. Soil Biol. Biochem. 52, 29–32.
Kastl, G.J., Fisher, I.H., Jegatheesan, V., 1999. Evaluation of chlorine decay kinetics expressions for drinking water distribution systems modelling. J. Water Supply: Res. Technol.-Aqua. 48 (6), 219–226.
Li, X.-F., Mitch, W.A., 2018. Drinking water disinfection byproducts (DBPs) and Human health effects: multidisciplinary challenges and opportunities. Env. Sci. Technol. 52 (4), 1681–1689.
McDonough, L.K., Andersen, M.S., Behnke, M.I., Rutlidge, H., Oudone, P., Meredith, K., O'Carroll, D.M., Santos, I.R., Marjo, C.E., Spencer, R.G.M., McKenna, A.M., Baker, A., 2022. A new conceptual framework for the transformation of groundwater dissolved organic matter. Nat Commun. 13 (1), 2153.
Mitch, W.A., Richardson, S.D., Zhang, X., Gonsior, M., 2023. High-molecular-weight by-products of chlorine disinfection. Nat. Water. 1 (4), 336–347.
Nihemaiti, M., Icker, M., Seiwert, B., Reemtsma, T., 2023. Revisiting disinfection byproducts with supercritical fluid chromatography-high resolution-mass spectrometry: identification of novel halogenated sulfonic acids in disinfected drinking water. Env. Sci. Technol. 57 (9), 3527–3537.
Nikolaou, A.D., Golfinopoulos, S.K., Lekkas, T.D., Kostopoulou, M.N., 2004. DBP levels in chlorinated drinking water: effect of humic substances. Env. Monit Assess 93 (1), 301–319.
Postigo, C., Andersson, A., Harir, M., Bastviken, D., Gonsior, M., Schmitt-Kopplin, P., Gago-Ferrero, P., Ahrens, L., Ahrens, L., Wiberg, K., 2021. Unraveling the chemodiversity of halogenated disinfection by-products formed during drinking water treatment using target and non-target screening tools. J. Hazard. Mater. 401, 123681.
Reemtsma, T., 2009. Determination of molecular formulas of natural organic matter molecules by (ultra-) high-resolution mass spectrometry: status and needs. J. Chromatogr. A 1216 (18), 3687–3701.
Reemtsma, T., Berger, U., Arp, H.P.H., Gallard, H., Knepper, T.P., Neumann, M., Quintana, J.B., Voogt, P.d., 2016. Mind the gap: persistent and mobile organic compounds—Water contaminants that slip through. Env. Sci. Technol. 50 (19), 10308–10315.
Richardson, S.D., Plewa, M.J., 2020. To regulate or not to regulate? What to do with more toxic disinfection by-products? J. Environ. Chem. Eng. 8 (4), 103939.
Richardson, S.D., Plewa, M.J., Wagner, E.D., Schoeny, R., DeMarini, D.M., 2007. Occurrence, genotoxicity, and carcinogenicity of regulated and emerging disinfection by-products in drinking water: a review and roadmap for research. Mutat. Res./Rev. Mutat. Res. 636 (1), 178–242.
Roth, V.-N., Lange, M., Simon, C., Hertkorn, N., Bucher, S., Goodall, T., Griffiths, R.I., Mellado-Vázquez, P.G., Mommer, L., Oram, N.J., Weigelt, A., Dittmar, T., Gleixner, G., 2019. Persistence of dissolved organic matter explained by molecular changes during its passage through soil. Nat. Geosci. 12 (9), 755–761.
Rougé, V., Allard, S., Croué, J.-P., von Gunten, U., 2018. In situ formation of free chlorine during ClO2 treatment: implications on the formation of disinfection byproducts. Env. Sci. Technol. 52 (22), 13421–13429.
USEPA (2003) Method 5030C (SW-846): purge-and-trap for aqueous samples, revision 3. Washington, DC. https://www.epa.gov/sites/default/files/2015-12/documents/5030c.pdf.
USEPA (2018) Method 8260D (SW-846): volatile organic compounds by gas chromatography/mass spectrometry (GC/MS), revision 4. Washington, DC. https://www.epa.gov/sites/default/files/2018-06/documents/method_8260d_update_vi_final_06-11-2018.pdf.
Wagner, E.D., Plewa, M.J., 2017. CHO cell cytotoxicity and genotoxicity analyses of disinfection by-products: an updated review. J. Environ. Sci. 58, 64–76.
Wang, D., Chen, X., Luo, J., Shi, P., Zhou, Q., Li, A., Pan, Y., 2024. Comparison of chlorine and chlorine dioxide disinfection in drinking water: evaluation of disinfection byproduct formation under equal disinfection efficiency. Water Res. 260, 121932.
Wawryk, N.J.P., Craven, C.B., Blackstock, L.K.J., Li, X.-F., 2021. New methods for identification of disinfection byproducts of toxicological relevance: progress and future directions. J. Environ. Sci. 99, 151–159.
Weishaar, J.L., Aiken, G.R., Bergamaschi, B.A., Fram, M.S., Fujii, R., Mopper, K., 2003. Evaluation of specific ultraviolet absorbance as an indicator of the chemical composition and reactivity of dissolved organic carbon. Env. Sci. Technol. 37 (20), 4702–4708.
Weisman, R.J., Heinrich, A., Letkiewicz, F., Messner, M., Studer, K., Wang, L., Regli, S., 2022. Estimating national exposures and potential bladder cancer cases associated with chlorination DBPs in U.S. Drinking water. Env. Health Perspect. 130 (8), 087002.
White, G.C., 2010. White's Handbook of Chlorination and Alternative Disinfectants. John Wiley & Sons.
Wright, J.M., Evans, A., Kaufman, J.A., Rivera-Núñez, Z., Narotsky, M.G., 2017. Disinfection by-product exposures and the risk of specific cardiac birth defects. Env. Health Perspect 125 (2), 269–277.
Wullenweber, J., Bennert, J., Mantel, T., Ernst, M., 2024. Characterizing macroporous ion exchange membrane adsorbers for natural organic matter (NOM) removal—Adsorption and regeneration behavior. Membr. (Basel) 14 (6), 124.
Wurz, J., Groß, A., Franze, K., Lechtenfeld, O., 2024. Lambda-miner: enhancing reproducible natural organic matter data processing with a semi-automatic web application. In: EGU General Assembly 2024. Vienna, Austria, 14–19 Apr 2024.
Zahn, D., Meusinger, R., Frömel, T., Knepper, T.P., 2019. Halomethanesulfonic acids—A new class of polar disinfection byproducts: standard synthesis, occurrence, and indirect assessment of mitigation options. Env. Sci. Technol. 53 (15), 8994–9002.